

# Global mass of buoyant marine plastics dominated by large long-lived debris

Received: 15 August 2022

Accepted: 26 May 2023

Published online: 7 August 2023

 Check for updates

Mikael L. A. Kaandorp<sup>1,2</sup>✉, Delphine Lobelle<sup>1</sup>, Christian Kehl<sup>1</sup>,  
Henk A. Dijkstra<sup>1</sup> & Erik van Sebille<sup>1</sup>

The fate of plastics that enter the ocean is a longstanding puzzle. Recent estimates of the oceanic input of plastic are one to two orders of magnitude larger than the amount measured floating at the surface. This discrepancy could be due to overestimation of input estimates, processes removing plastic from the surface ocean or fragmentation and degradation. Here we present a 3D global marine mass budget of buoyant plastics that resolves this discrepancy. We assimilate observational data from different marine reservoirs, including coastlines, the ocean surface, and the deep ocean, into a numerical model, considering particle sizes of 0.1–1,600.0 mm. We find that larger plastics (>25 mm) contribute to more than 95% of the initially buoyant marine plastic mass: 3,100 out of 3,200 kilotonnes for the year 2020. Our model estimates an ocean plastic input of about 500 kilotonnes per year, less than previous estimates. Together, our estimated total amount and annual input of buoyant marine plastic litter suggest there is no missing sink of marine plastic pollution. The results support higher residence times of plastics in the marine environment compared with previous model studies, in line with observational evidence. Long-lived plastic pollution in the world's oceans, which our model suggests is continuing to increase, could negatively impact ecosystems without countermeasures and prevention strategies.

An estimated 250 metric kilotonnes (250 million kilograms) of plastic pollution floats on the surface of the global ocean<sup>1,2</sup>. A much larger amount of plastic pollution is estimated to enter the ocean every year, on the order of 800–2,400 kilotonnes from rivers<sup>3</sup> and 4,800–23,000 kilotonnes from coastal regions<sup>4,5</sup> (see Extended Data Fig. 1). We assess what causes the misalignment between the estimated plastic input and the total floating plastic mass by assimilating unprecedented amounts of observational data into a state-of-the-art three-dimensional (3D) global transport model for marine plastics, considering timescales on the order of decades (1980–2020). Our dataset includes concentrations in terms of both number (in  $n\text{ m}^{-3}$  in the ocean and  $n\text{ m}^{-1}$  on beaches) and mass (in  $\text{g m}^{-3}$  in the ocean and  $\text{g m}^{-1}$  on beaches). In total, we use 14,977 measurements from the surface water, 7,114 from beaches and 120 from the deep ocean (for an overview, see Extended Data Fig. 2 and Extended

Data Table 1). From 2,303 beach measurements, we additionally use the fraction of fishing-related items such as fishing nets. We expand on previous mass budget studies<sup>6</sup> by increasing the model complexity, incorporating numerous recently developed models for different processes affecting marine plastic transport: sinking via biofouling, beaching, turbulent vertical mixing and fragmentation. By using a Bayesian framework, our model results match well with both observed plastic concentrations across different marine reservoirs and different size classes (Extended Data Fig. 3) and the latest understanding of processes removing plastic from the surface ocean.

Sinking of plastic particles probably plays an important role in removing plastic mass from the surface water<sup>6–8</sup>. Initially buoyant items can start sinking due to the growth of biofilm on their surface, on timescales of weeks to months<sup>9–11</sup>. We consider various biofouling

<sup>1</sup>Institute for Marine and Atmospheric Research Utrecht, Department of Physics, Utrecht University, Utrecht, the Netherlands. <sup>2</sup>Forschungszentrum Jülich GmbH, Institute of Bio- and Geosciences, IBG-3 (Agrosphere), Jülich, Germany. ✉e-mail: [m.kaandorp@fz-juelich.de](mailto:m.kaandorp@fz-juelich.de)

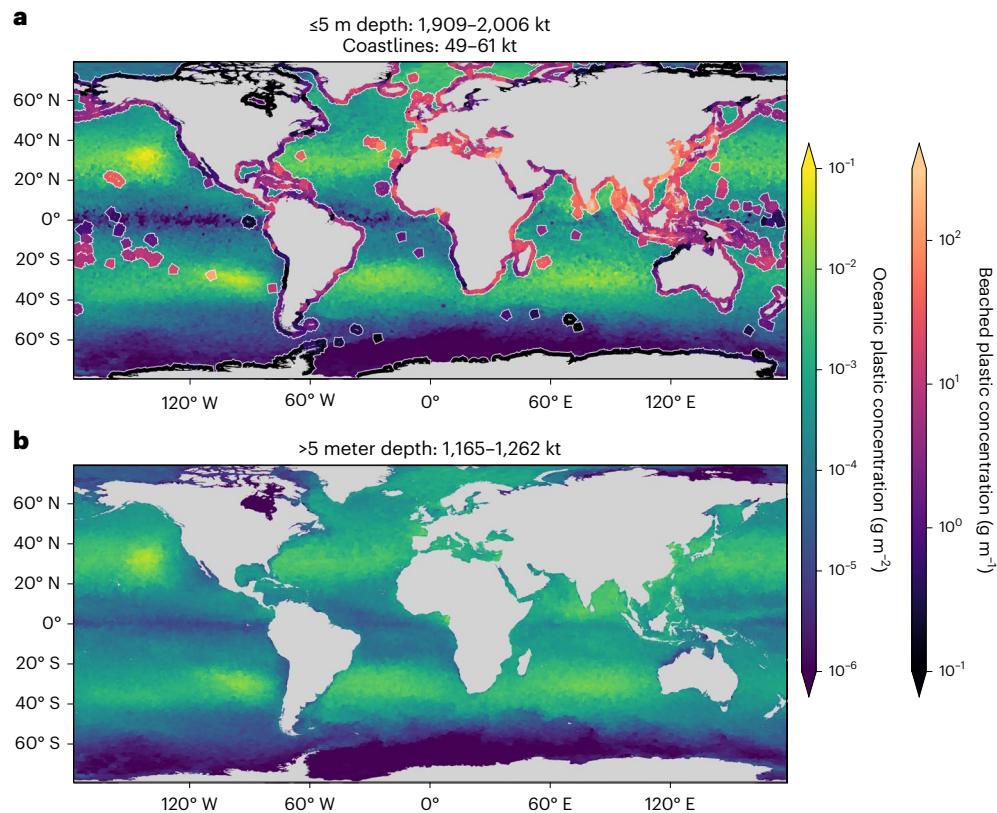


**Fig. 1** A map of the predicted plastic concentrations in the marine environment. **a,b**, The predicted concentrations ( $\text{g m}^{-2}$ ) of plastic items (0.1–1,600.0 mm) are shown for the most likely parameter estimates in the ocean

surface (0–5 m depth) (**a**) and below the ocean surface (**b**). Predicted plastic concentrations on beaches (in purple to red in **a**, white delineation) are shown in terms of  $\text{g m}^{-1}$ . The estimated concentrations are shown for the year 2020.

scenarios, including fouling–defouling cycles<sup>12,13</sup>. Model studies<sup>14,15</sup> have suggested that the majority (67–77%) of plastics reside on beaches or in coastal waters up to 10 km offshore. We therefore include models for beaching and resuspension of plastics back to the ocean<sup>16</sup>. Surface measurements are currently the only large global observational datasets available in the ocean. Mixing of plastic particles in the water column is hypothesized to be an explanation for the relatively low estimates of plastic mass found in surface net trawls<sup>13,17</sup>. We account for this by resolving plastic transport three dimensionally, including the modelling of vertical turbulent mixing in the water column<sup>18</sup>.

Fragmentation plays an important role in explaining the increasing number of plastic particles for smaller particle sizes<sup>19,20</sup> and can furthermore affect mass budget analyses by breaking down plastic items into particles smaller than typically measured sizes<sup>21</sup>. We therefore use a recently developed fragmentation model<sup>21</sup>, including a size spectrum of plastic particles (0.1–1,600.0 mm). This allows us to assimilate different types of observations such as net trawls that capture mainly microplastics ( $< 5$  mm, with a typical mesh size of 0.2 mm (ref. 22)), as well as measurements of larger plastics ( $> 25$  mm) from shipboard observations and beach clean-up campaigns. With this size spectrum, we can also more accurately link concentrations in terms of number of plastic particles to concentrations in terms of plastic mass, as a biased conversion between the two has been shown to have a big impact on mass budget estimates<sup>23</sup>.

We focus on plastics that are initially buoyant when entering the marine environment, such as polyethylene, polypropylene and polystyrene. These polymers have been shown to make up the majority of items in the ocean's surface<sup>24</sup>, deeper layers<sup>25</sup> and beaches<sup>26–28</sup>. This means we do not consider polymers denser than seawater such as polyvinyl chloride and polyethylene terephthalate, which are estimated to make up about 35–40% of the plastic mass entering the marine environment<sup>6,29,30</sup>.

### A 3D map of marine plastic litter

We estimate a total amount of initially buoyant plastics in the 3D global ocean of 3,200 kilotonnes (95% confidence interval: 3,000–3,400 kilotonnes) for the year 2020 on the basis of our assimilated model. A 3D global map of the estimated marine plastic pollution for the complete modelled particle size spectrum (0.1–1,600.0 mm) is shown in Fig. 1. The largest fraction of plastic mass is located at the ocean surface: 59–62%. More than a third of the mass resides deeper in the ocean (36–39%) and the remainder is located on beaches (1.5–1.9%).

These results, as well as the the estimated fluxes into and out of the marine environment, are summarized in the schematic overview in Fig. 2. We calculate a total marine plastic input of 500 kilotonnes per year (95% confidence interval: 470–540 kilotonnes for the reference year 2020), originating from coastlines (39–42%), from fishing activity (45–48%) and from rivers (12–13%). The total input we predict increases by about 4% per year, which is consistent with the estimated increase in global plastic waste generation of about 5% per year (ref. 31) and with the observed increase of plastic concentrations in the Pacific Ocean<sup>30</sup> and the North Atlantic Ocean<sup>32</sup>. Our calculated global riverine input of 57–69 kilotonnes per year is lower than previous estimates (800–2,700 kilotonnes per year (ref. 3)). The 190–220 kilotonnes of input from coastlines is furthermore at least an order of magnitude smaller than previous estimates (4,800–12,700 kilotonnes per year (ref. 4)). These much lower input estimates for rivers and coastlines are consistent with recent modelling and observational studies<sup>6,23,33,34</sup>. The estimated input of 220–260 kilotonnes from fishing activity is somewhat lower than previous estimates of 640 kilotonnes per year<sup>35</sup>. Our modelled concentrations of fishing-related plastics are consistent with the observed amount of items on beaches (Supplementary Information section 1.2) and match qualitatively with review studies showing that the majority of plastic litter in the

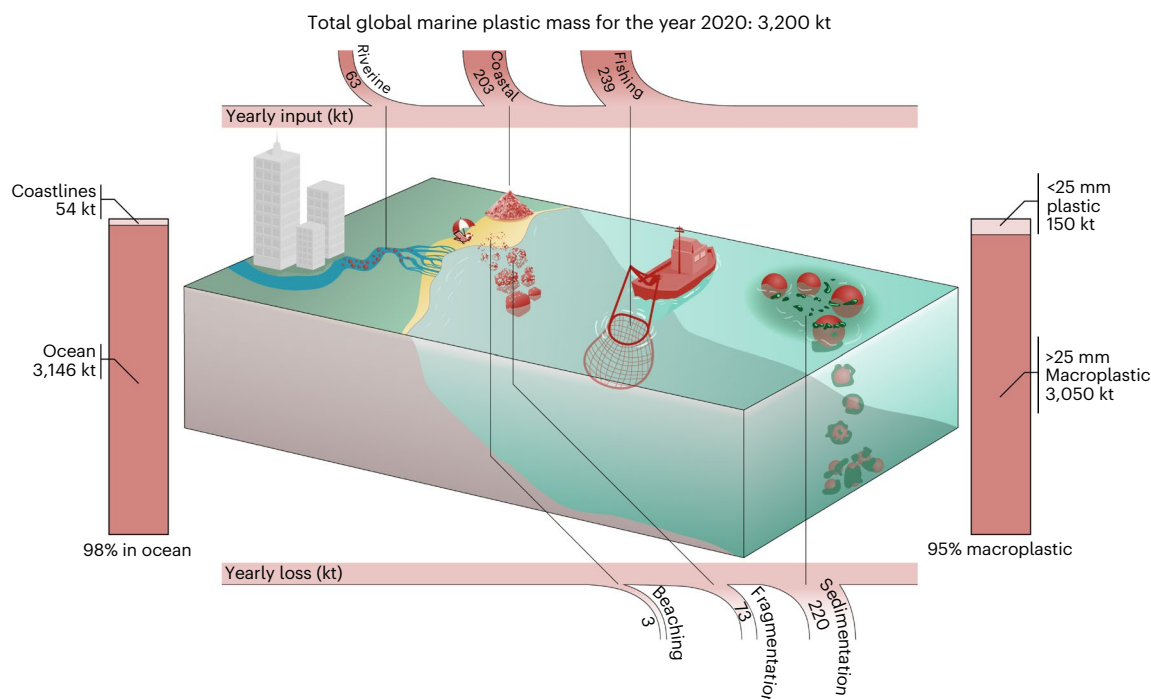


**Fig. 2 | Schematic overview of the estimated marine plastic fluxes and standing stocks.** Fluxes (top and bottom) are given in kilotonnes per year; standing stocks (left and right) are given in kilotonnes. Sizes of objects are not to scale. Fragmentation loss is defined as particles becoming smaller than 0.1 mm. Credit: [thisillustrations.com](https://thisillustrations.com).

open ocean originates from the ocean<sup>36</sup> (for example, items such as nets, ropes and buoys).

Biological processes (such as biofouling) play an important role in the dynamics and export of plastic waste from the ocean surface. We estimate that 220 kilotonnes of plastics are exported to marine sediments per year, of which 6 kilotonnes are microplastics (<5 mm), which is close to the 7–420 kilotonnes of microplastics per year from previous modelling studies<sup>7</sup>. We estimate that 6,200 kilotonnes of initially buoyant plastics have ended up in marine sediments since 1950, which is less than a recent estimate of 25,000–900,000 kilotonnes (ref. 8) for all plastic (buoyant and non-buoyant). Plastic items with densities higher than seawater are not accounted for in our model, and hence sedimentation fluxes near source regions may be underestimated considerably. Our model shows that about half of the initially buoyant plastic particles in the marine environment experience so much biofouling that they start sinking or become neutrally buoyant. The large quantity of plastic particles in the deep ocean<sup>25</sup>, for a large part consisting of low-density polymers such as polyethylene and polypropylene, cannot be explained without this fouling.

We estimate a plastic sink of three kilotonnes per year at coastlines due to processes such as burial, clean-up efforts and direct ultraviolet degradation. In addition, a substantial amount of plastics are fragmented into particles smaller than 0.1 mm—about 73 kilotonnes per year. We estimate that 2.2% of plastics larger than 5 mm fragment into particles smaller than 5 mm per year, which is very close to previous model estimates of about 3% per year (ref. 14).

### Dominant contribution of large plastic items

One of our key results is that the majority of plastic mass is contained in the large plastic items (>25 mm): 90–98% (2,800–3,300 kilotonnes). Microplastics (<5 mm) and plastics between 5 and 25 mm form the small remainder at 49–53 kilotonnes and 150–170 kilotonnes, respectively, which is on the same order of magnitude as previous estimates for small (0.3–200.0 mm) floating plastics (93–236 kilotonnes<sup>2</sup>). These findings

are also consistent with an analysis of the Great Pacific Garbage Patch<sup>30</sup>, where it was found that microplastics (<5 mm) make up only 8% of the total plastic mass at the ocean surface.

Particle size distributions (Fig. 3a) reveal an increase in the total plastic mass with particle size according to a power law, up to an estimated dominant particle size of about 0.4 metres. Few particles above this length scale are expected to enter the marine environment. The model results indicate that most of the plastic mass for particles smaller than 0.8 mm is below the ocean surface. The total plastic mass on coastlines is about an order of magnitude less compared with the surface and deep ocean for all particle sizes. The number of particles increases for decreasing particle size (Fig. 3b) according to a power law, as has been shown in previous observational studies<sup>19,37</sup>.

Our estimate of the total buoyant plastic mass for particles smaller than 5 mm (51 kilotonnes) is similar to previous studies (35.5 kilotonnes<sup>1</sup>). However, our mass estimate for particles between 5 and 200 mm, 700 kilotonnes, is much higher than previously estimated (30.6 kilotonnes (ref. 1)). This is even more so for particles larger than 200 mm, where our estimate of 2,500 kilotonnes vastly exceeds the previously estimated 202.8 kilotonnes (ref. 1). This difference can be explained largely by the very broad size intervals used previously<sup>1</sup>.

As an example, it can be seen in Fig. 3 (left panel) that the larger particles around 200 mm by far dominate the total mass in the size range 4.76–200.00 mm, whereas these particles are very sparse in terms of total number (right panel). These large particles are therefore likely to be undersampled, causing an underestimation of the total mass. Biases in mass budget estimates due to incorrect usage of mean particle masses were also observed for riverine plastic studies<sup>23</sup>. The large differences in total mass estimates underline the importance of treating different particle sizes very carefully in mass budget studies: preferably a (semi-) continuous size spectrum should be used.

We recommend that future plastic measurement campaigns and mass budget studies treat number and mass measurements more carefully. The amount of plastic particles increases exponentially for

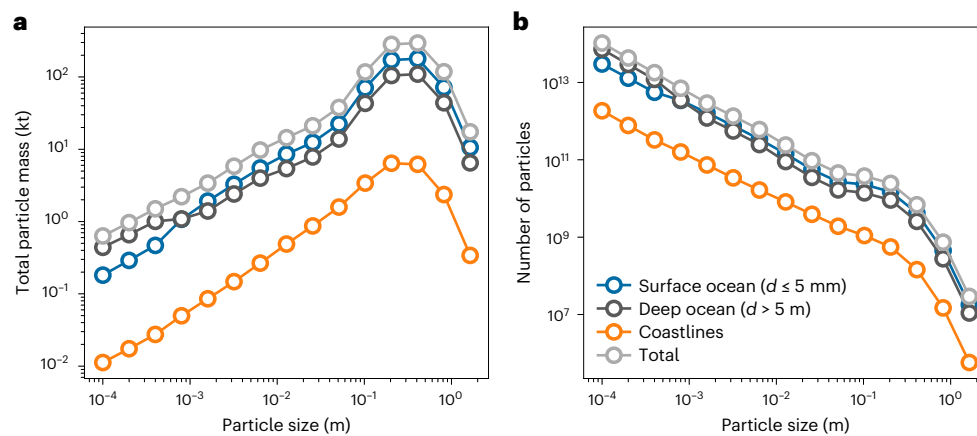


**Fig. 3 | Particle size distributions of marine plastics. a, b,** The total mass in kilotonnes (a) and number of particles (b) for different size classes (from 0.1 to 1,600.0 mm diameter). Note the logarithmic axes.

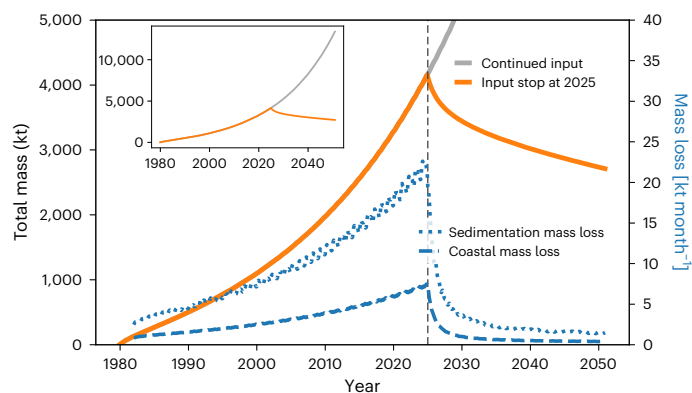


**Fig. 4 | Scenarios for the future marine plastic mass budget.** A scenario for a sudden stop of new plastics introduced into the marine environment in 2025 is shown in orange, a business-as-usual scenario with an exponentially increasing input in grey. The inset presents a zoom out of both scenarios. Also shown are the expected marine plastic mass losses along coastlines (dashed blue line) and due to sedimentation (dotted blue line), showing that the mass loss after a sudden input stop is expected to decrease rapidly.

decreasing particle sizes. Reporting the number of particles in observational studies can be unreliable when no strict lower limit of the particle size is used. This is especially true for visual observations (the main source of data for beaches<sup>38,39</sup>) as the lower detection limit probably varies per person. Measuring the total mass of items is more reliable in those cases as most of the plastic mass in the marine environment is contained in the larger particle sizes, which are more easily observed.

### Implications of residence times for future projections

In summary, we find that the total amount of buoyant marine plastic litter, 3,000–3,400 kilotonnes, is much higher than previous estimates<sup>1</sup>, which for a large part can be explained by better representing large plastic object masses. We also find a plastic input into the marine environment of 470–540 kilotonnes per year, at least an order of magnitude less than previous estimates<sup>3–5</sup>. The decreased input and increased standing stock suggest that there is no ‘missing sink’ for marine plastic pollution, which has been the focus of many recent papers<sup>7,23,33,40</sup>. Our mass budget estimate is consistent with observed plastic concentrations in different marine reservoirs and with our latest understanding

of processes removing plastic particles from the surface ocean, such as biofouling and sedimentation, beaching, fragmentation and mixing.

Our finding of a lower plastic input into the marine environment and a higher standing stock means that the residence time of plastics in the marine environment is much higher than previously estimated. For example, some studies<sup>41</sup> predicted that given an instantaneous stop of plastic emissions, more than 95% of the plastic mass would be removed from the ocean surface within 1–2 years due to fragmentation and sinking. We show a similar analysis for a sudden stop of new plastics introduced into the marine environment in 2025 in Fig. 4 using our data-assimilated model. We expect that in this scenario only 10% of the plastic mass would be removed from the marine environment within 2 years (orange line). The removal rate is expected to decrease rapidly over time as plastics move from coastal regions to the subtropical gyres. As there is no beaching and little sinking of marine plastics in these low algal areas compared with coastal waters<sup>11,13</sup>, the plastic particles become highly persistent (Supplementary Information section 1.3).

We estimate that the plastic input into the marine environment is probably still growing around 4% per year. Previous studies<sup>42</sup> found no conclusive temporal trends regarding the amount of plastic litter in the marine environment. Establishing temporal trends is difficult due to the high variance in measured plastic concentrations<sup>43</sup>. Our estimated growth rate of 4% per year gives the best match with observational data over the past decades (Supplementary Information section 1.5) but might change in the future under the influence of mitigation strategies and clean-up efforts. Without further mitigation strategies and clean-up efforts, our estimated growth rate of 4% per year has the potential to double the plastic standing stock within two decades, as shown in the inset in Fig. 4. The combination of a projected exponentially increasing input and long persistence of marine plastics means a likely increasing negative impact of marine plastic pollution on ecosystems in the future.

### Online content

Any methods, additional references, Nature Portfolio reporting summaries, source data, extended data, supplementary information, acknowledgements, peer review information; details of author contributions and competing interests; and statements of data and code availability are available at <https://doi.org/10.1038/s41561-023-01216-0>.

### References

- Eriksen, M. et al. Plastic pollution in the world's oceans: more than 5 trillion plastic pieces weighing over 250,000 tons afloat at sea. *PLoS ONE* **9**, 0111913 (2014).

2. van Sebille, E. et al. A global inventory of small floating plastic debris. *Environ. Res. Lett.* **10**, 124006 (2015).
3. Meijer, L. J. J., van Emmerik, T., van der Ent, R., Schmidt, C. & Lebreton, L. More than 1000 rivers account for 80% of global riverine plastic emissions into the ocean. *Sci. Adv.* **7**, eaz5803 (2021).
4. Jambeck, J. R. et al. Plastic waste inputs from land into the ocean. *Science* **347**, 768–771 (2015).
5. Borrelle, S. B. et al. Predicted growth in plastic waste exceeds efforts to mitigate plastic pollution. *Science* **369**, 1515–1518 (2020).
6. Kaandorp, M. L. A., Dijkstra, H. A. & van Sebille, E. Closing the Mediterranean marine floating plastic mass budget: inverse modeling of sources and sinks. *Environ. Sci. Technol.* **54**, 11980–11989 (2020).
7. Kvale, K. F., Prowe, A. E. F. & Oschlies, A. A critical examination of the role of marine snow and zooplankton fecal pellets in removing ocean surface microplastic. *Front. Mar. Sci.* **6**, 00808 (2020).
8. Martin, C., Young, C. A., Valluzzi, L. & Duarte, C. M. Ocean sediments as the global sink for marine micro- and mesoplastics. *Limnol. Oceanogr. Lett.* <https://doi.org/10.1002/lol2.10257> (2022).
9. Ye, S. & Andrady, A. L. Fouling of floating plastic debris under Biscayne Bay exposure conditions. *Mar. Pollut. Bull.* **22**, 608–613 (1991).
10. Fazole, F. M. C. & Ryan, P. G. Biofouling on buoyant marine plastics: an experimental study into the effect of size on surface longevity. *Environ. Pollut.* **210**, 354–360 (2016).
11. Lobelle, D. et al. Global modeled sinking characteristics of biofouled microplastic. *J. Geophys. Res. Oceans* **126**, e2020JC017098 (2021).
12. Kooi, M., Van Nes, E. H., Scheffer, M. & Koelmans, A. A. Ups and downs in the ocean: effects of biofouling on vertical transport of microplastics. *Environ. Sci. Technol.* **51**, 7963–7971 (2017).
13. Fischer, R. et al. Modelling submerged biofouled microplastics and their vertical trajectories. *Biogeosciences* **19**, 2211–2234 (2022).
14. Lebreton, L., Egger, M. & Slat, B. A global mass budget for positively buoyant macroplastic debris in the ocean. *Sci. Rep.* **9**, 12922 (2019).
15. Onink, V., Jongedijk, C., Hoffman, M., van Sebille, E. & Laufkötter, C. Global simulations of marine plastic transport show plastic trapping in coastal zones. *Environ. Res. Lett.* <https://doi.org/10.1088/1748-9326/abecbd> (2021).
16. Onink, V., Wichmann, D., Delandmeter, P. & van Sebille, E. The role of Ekman currents, geostrophy, and Stokes drift in the accumulation of floating microplastic. *J. Geophys. Res. Oceans* **124**, 1474–1490 (2019).
17. Poulain, M. et al. Small microplastics as a main contributor to plastic mass balance in the North Atlantic Subtropical Gyre. *Environ. Sci. Technol.* **53**, 1157–1164 (2019).
18. Onink, V., van Sebille, E. & Laufkötter, C. Empirical Lagrangian parametrization for wind-driven mixing of buoyant particles at the ocean surface. *Geosci. Model Dev.* **15**, 1995–2012 (2022).
19. Cózar, A. et al. Plastic debris in the open ocean. *Proc. Natl Acad. Sci. USA* **111**, 10239–10244 (2014).
20. Song, Y. K. et al. Combined effects of UV exposure duration and mechanical abrasion on microplastic fragmentation by polymer type. *Environ. Sci. Technol.* **51**, 4368–4376 (2017).
21. Kaandorp, M. L. A., Dijkstra, H. A. & van Sebille, E. Modelling size distributions of marine plastics under the influence of continuous cascading fragmentation. *Environ. Res. Lett.* **16**, 54075 (2021).
22. Cózar, A. et al. Plastic accumulation in the Mediterranean Sea. *PLoS ONE* **10**, 0121762 (2015).
23. Weiss, L. et al. The missing ocean plastic sink: gone with the rivers. *Science* **111**, 107–111 (2021).
24. Bond, T., Ferrandiz-mas, V., Felipe-sotelo, M. & van Sebille, E. The occurrence and degradation of aquatic plastic litter based on polymer physicochemical properties: a review. *Crit. Rev. Environ. Sci. Technol.* **48**, 685–722 (2018).
25. Egger, M., Sulu-Gambari, F. & Lebreton, L. First evidence of plastic fallout from the North Pacific Garbage Patch. *Sci. Rep.* **10**, 7495 (2020a).
26. Vianello, A. et al. Microplastic particles in sediments of Lagoon of Venice, Italy: first observations on occurrence, spatial patterns and identification. *Estuar. Coast. Shelf Sci.* **130**, 54–61 (2013).
27. Frias, J. P. G. L., Otero, V. & Sobral, P. Evidence of microplastics in samples of zooplankton from Portuguese coastal waters. *Mar. Environ. Res.* **95**, 89–95 (2014).
28. Carson, H. S., Colbert, S. L., Kaylor, M. J. & McDermid, K. J. Small plastic debris changes water movement and heat transfer through beach sediments. *Mar. Pollut. Bull.* **62**, 1708–1713 (2011).
29. Andrady, A. L. Microplastics in the marine environment. *Mar. Pollut. Bull.* **62**, 1596–1605 (2011).
30. Lebreton, L. et al. Evidence that the Great Pacific Garbage Patch is rapidly accumulating plastic. *Sci. Rep.* **8**, 4666 (2018).
31. Geyer, R., Jambeck, J. R. & Law, K. L. Production, use, and fate of all plastics ever made. *Sci. Adv.* **3**, 19–24 (2017).
32. Wilcox, C., Hardesty, B. D. & Law, K. L. Abundance of floating plastic particles is increasing in the western North Atlantic Ocean. *Environ. Sci. Technol.* **54**, 790–796 (2020).
33. Ryan, P. G., Weideman, E. A., Perold, V. & Moloney, C. L. Toward balancing the budget: surface macro-plastics dominate the mass of particulate pollution stranded on beaches. *Front. Mar. Sci.* **7**, 575395 (2020).
34. Schöneich-Argent, R. I., Dau, K. & Freund, H. Wasting the North Sea? A field-based assessment of anthropogenic macrolitter loads and emission rates of three German tributaries. *Environ. Pollut.* **263**, 114367 (2020).
35. Li, W. C., Tse, H. F. & Fok, L. Plastic waste in the marine environment: a review of sources, occurrence and effects. *Sci. Total Environ.* **566–567**, 333–349 (2016).
36. Morales-Caselles, C. et al. An inshore–offshore sorting system revealed from global classification of ocean litter. *Nat. Sustain.* **4**, 484–493 (2021).
37. Kooi, M. & Koelmans, A. A. Simplifying microplastic via continuous probability distributions for size, shape, and density. *Environ. Sci. Technol. Lett.* **6**, 551–557 (2019).
38. *Guideline for Monitoring Marine Litter on the Beachs in the OSPAR Maritime Area* (OSPAR, 2010).
39. Burgess, H. K., Herring, C. E., Lippiatt, S., Lowe, S. & Uhrin, A. V. *NOAA Marine Debris Monitoring and Assessment Project Shoreline Survey Guide Technical Memorandum NOS OR&R 56* (NOAA, 2021).
40. Atsuhiko, I. & Iwasaki, S. The fate of missing ocean plastics: are they just a marine environmental problem? *Sci. Total Environ.* **825**, 153935 (2022).
41. Koelmans, A. A., Kooi, M., Law, L. & van Sebille, E. All is not lost: deriving a top-down mass budget of plastic at sea. *Environ. Res. Lett.* <https://doi.org/10.1088/1748-9326/aa9500> (2017).
42. Galgani, F. et al. Are litter, plastic and microplastic quantities increasing in the ocean? *Microplast. Nanoplast.* **1**, 8–11 (2021).
43. de Haan, W. P., Sanchez-Vidal, A. & Canals, M. Floating microplastics and aggregate formation in the Western Mediterranean Sea. *Mar. Pollut. Bull.* **140**, 523–535 (2019).

**Publisher's note** Springer Nature remains neutral with regard to jurisdictional claims in published maps and institutional affiliations.

**Open Access** This article is licensed under a Creative Commons Attribution 4.0 International License, which permits use, sharing, adaptation, distribution and reproduction in any medium or format, as long as you give appropriate credit to the original author(s) and the source, provide a link to the Creative Commons license, and indicate if changes were made. The images or other third party material in this article are included in the article's Creative Commons license, unless indicated otherwise in a

credit line to the material. If material is not included in the article's Creative Commons license and your intended use is not permitted by statutory regulation or exceeds the permitted use, you will need to obtain permission directly from the copyright holder. To view a copy of this license, visit <http://creativecommons.org/licenses/by/4.0/>.

© The Author(s) 2023

## Methods

We use a hybrid Lagrangian–Eulerian model to efficiently advect a virtual plastic tracer through the global ocean, under various environmental forcings. First, we use Lagrangian simulations to advect a globally dense set of virtual plastic particles over a time span of one month. We run simulations for different particle sizes, different biofouling scenarios and different months. We then use each of these simulations to construct transition matrices: linear systems that define the probability that plastic particles move from one grid cell of the ocean to another<sup>44,45</sup>. Parameterized sources and sinks for marine plastic pollution are then directly added into the transition matrix model. This allows us to efficiently evaluate different source and sink scenarios, which is necessary during the data assimilation step where we calibrate the set of unknown parameters to optimally match the observational data. For a more detailed explanation, see Supplementary Information (section 2.4). With the hybrid Lagrangian–Eulerian approach, we have a parsimonious model that can explain the sparse observed data with as few parameters as possible (16 in total; Supplementary Fig. 5).

### Data assimilation

Parameters defining sources, transport and sinks of plastic pollution are given a plausible range (the Bayesian ‘prior’) in accordance with current understanding of these processes as discussed in the next sections. Gaussian probability density functions are used to define the ranges, where the 95% confidence intervals define the lower and upper parameter estimates. Measurements contain an error due to both instrument errors (for example, differences between campaigns in sampling) and representation errors (for example, due to unresolved scales and processes<sup>46</sup>). Measurement error is estimated by calculating variograms of the observational data<sup>6,47</sup>. We use an ensemble smoother with multiple data assimilation to update the model parameter values with the observational data<sup>48</sup>. An ensemble of 55 members (iterated 8 times) is used to estimate the most likely posterior parameter values and confidence intervals. The ensemble members are furthermore used to quantify uncertainty ranges for the estimated plastic concentrations and fluxes. The modelled plastic concentrations represent a mean state, where subgrid-scale variability is not captured. We estimate the subgrid-scale variability from the model–observation mismatch after the data assimilation procedure. The subgrid-scale variability is accounted for in the uncertainty ranges by performing a Monte Carlo analysis<sup>6</sup>, where the plastic concentrations in each ensemble member are perturbed 100 times.

### Lagrangian model

To generate the transition matrices, we advect virtual plastic particles three dimensionally in the global ocean using OceanParcels<sup>49</sup>, with the Mercator Ocean PSY4 analysis product at 1/12° resolution as forcing<sup>50</sup>. This forcing product has been assimilated with various data sources (including altimetry, sea surface temperature, salinity and temperature vertical profile data) and includes freshwater fluxes<sup>51</sup>. Particles are released horizontally on a hexagonal grid with an average hexagon edge length of 22 km and vertically at 12 logarithmically spaced depth layers between 0.5 m and 5,000 m. This release is repeated every month for five years (2015–2019). Transport is resolved for six different particle sizes (diameter) using an increment of a factor 4 (0.1 mm, 0.4 mm, 1.6 mm, 6.4 mm, 26 mm, 102 mm). These particles experience a varying amount of influence from vertical turbulent mixing, which can affect their horizontal dispersion<sup>52</sup>. Analysis showed that of these sizes, the largest particles (102 mm) experience negligible effect from vertical mixing in the water column due to their high buoyancy. This is therefore the largest particle size for which we calculate the advection in OceanParcels. We assume similar transport for larger particles (up to 1.6 m) when constructing the transition matrices (‘Transition matrix model’ section) since these all remain at the ocean surface. Recent studies have shown that simply adding the Stokes drift velocity<sup>53</sup> or a windage term<sup>30</sup> to Lagrangian particle simulations representing plastic transport does

not increase the match with observational data, which was verified in a preliminary analysis. These effects are therefore not included in our model. Lagrangian particle simulations usually include a stochastic (diffusive) term<sup>54</sup> to account for missing subgrid-scale effects (for example, submesoscale eddies). This stochastic term is not included as the transition matrices calculated from the Lagrangian transport (‘Transition matrix model’ section) already introduce diffusion in the dynamics<sup>45</sup>. Transport is resolved for four different vertical transport scenarios under influence of turbulence and biofouling as described in the next section. The total number of particle trajectories across all simulations for the different months, sizes and transport scenarios is 1.7 billion.

**Vertical motions.** We consider four different scenarios for the vertical behaviour of plastic particles in the ocean. In all four scenarios, vertical diffusion due to turbulence is included, using a Markov-0 random walk model<sup>18</sup> forced by the PSY4 vertical diffusivity fields.

First, we consider plastic particles that remain positively buoyant, with a rise velocity that is dependent on the particle size<sup>17</sup>. Spherical particles<sup>55</sup> with a density of 1,010 kg m<sup>-3</sup> are used as a baseline, giving the best match with experimentally determined rise velocities of particles found in the marine environment (Supplementary Fig. 9). In reality, environmental plastics have a range of densities and shapes<sup>37</sup>. For a given particle size in the model, we take a linear combination of the six differently sized baseline particles to model an assemblage of particles with different rise velocities. This linear combination is calibrated during the data assimilation procedure to give an optimal match with the observational data (see the Supplementary Information section 2.3 for further details). Using spherical particles as a baseline keeps the rise velocity model consistent with our biofouling implementation<sup>13</sup> and keeps the calculation procedure computationally cheap (as opposed to some recent iterative procedures for calculating rise velocities of non-spherical particles<sup>17,56</sup> that would add extra computational costs).

Second, we include two scenarios for biofouling using a recently developed Lagrangian model<sup>13</sup>. Biochemistry fields from the Mercator Ocean BIOMER4 analysis product are used at 1/4° resolution. Biofilm on plastic particles is gained via collisions and growth with algae in this model and is lost via respiration. Biofilm loss via grazing and viral lysis is neglected to keep the amount of free model parameters limited since this effect is suggested to be minor<sup>13</sup>. Due to the growth and loss of biofilm, plastic particles can oscillate vertically in the water column. This potential oscillatory behaviour has not yet been experimentally observed. We therefore also include a scenario where the fouling of particles is permanent, neglecting the respiration loss term. In our fourth scenario, particles become neutrally buoyant due, for example, to a balance in the fouling and defouling processes or to slightly negatively buoyant particles reaching an equal-density isopycnal surface.

### Transition matrix model

The statistics of the Lagrangian particle transport (probabilities that particles move from one grid cell of the ocean to another) are stored in transition matrices, with time windows of 30 days. The Uber H3 grid is used to construct the transition matrix bins horizontally, where each cell has an edge length of approximately 60 km. Each horizontal bin is furthermore divided vertically into four depth bins, with boundaries at 0, 5, 50 and 500 m deep and at the ocean floor. Additional cells are introduced into the transition matrix system representing the coastline segments inside the coastal cells (Supplementary Fig. 11) to model transport between the ocean and beaches. The resulting transition matrices have a size of 121,000 × 121,000.

In the next two sections, we discuss how sources, transport and sinks of marine plastics are parameterized in the transition matrix model. We touch on plausible ranges for each parameter value as these are used to define the prior probability density functions in the Bayesian analysis when assimilating observational data into the model (Supplementary Information section 1.4).

**Parameterization of sources.** We consider three major types of marine plastic pollution sources in our model: rivers, coastlines and fishing activity<sup>30</sup>. For a global overview, see Extended Data Fig. 1.

Current estimates of riverine plastic inputs vary widely. Global estimates based on modelling studies calibrated to observational data range from 1,150–2,410 kilotonnes per year (ref. 57) to 800–2,700 kilotonnes per year (ref. 3). However, it was recently argued that these values might be overestimates<sup>23</sup>, giving a much lower estimate of about 6.1 kilotonnes per year. Reasons for potential overestimations are (1) biases in conversion from number concentrations to mass concentrations due to too-high particle mass estimates and (2) the mixing of different sampling techniques without accounting for varying lower size detection limits.

We use the most recent global estimate of riverine inputs<sup>3</sup>, given that they find a reasonable correlation to observational riverine data ( $R = 0.86$ ) and their data are publicly available. We take possible biases into account by scaling the total input with a factor  $S_{riv}$ , where the bounds of this prior are chosen to capture both the high-end (2,700 kilotonnes per year (ref. 3)) and low-end (6.1 kilotonnes per year (ref. 23)) estimates.

For coastal mismanaged plastic waste (MPW), we make use of a global MPW dataset per country<sup>4</sup> in terms of kilotonnes per year per capita. Combined with the estimated population density within 50 kilometres from the coast<sup>58</sup>, this gives us the coastal MPW per unit area per year. A parameter  $S_{pop}$ , defines the relative input of coastal MPW with respect to the total riverine input.

We estimate plastic loss per fishing hour by scaling a globally estimated fishing hours dataset<sup>59</sup> with a parameter  $S_{fis}$ , that defines the relative input of fishing-related plastic with respect to the total riverine input. The prior bounds for  $S_{pop}$  and  $S_{fis}$  are defined using previously estimated input ranges for different waste categories<sup>30</sup>. This gives 2.7–7.3 times the riverine input for coastal MPW and 0.2–2.0 times the riverine input for fishing-related plastic.

Larger items make up the majority of plastic mass found in the marine environment<sup>30,33</sup>, while small fragments dominate in terms of the number of particles<sup>22</sup>. It is not yet well known which particle size dominates new plastic items introduced into the marine environment. We parameterize the plastic input size using a log-normal distribution, capturing the dominant sizes of plastic packaging in municipal solid-waste sorting facilities (about 0.2 m (ref. 60)) and the dominant sizes of plastic items found in rivers (about 0.2–0.3 m (refs. 61,62)) (see Supplementary Information section 2.1 for more details).

Plastic waste generation has increased exponentially the past decades<sup>31</sup>. We use an exponential function to parameterize the possibility that this has led to an increasing amount of waste entering the ocean. The midpoint estimate for the exponential growth rate ( $GR_{in}$ ) prior is calibrated to plastic waste production estimates<sup>31</sup>, and the lower bound is set to zero to allow for the possibility of no increased input into the ocean (for example, due to more efficient collection and processing of waste).

**Parameterization of transport and sinks.** The four different vertical transport scenarios ('Vertical motions' section) yield four different transition matrices. We assume particles in the ocean are an assembly of these four scenarios. How much each scenario contributes is parameterized using three fractions— $f_{of}$  (oscillatory fouling/defouling),  $f_{pf}$  (permanent fouling) and  $f_{nb}$  (neutrally buoyant)—with the remaining fraction being the positively buoyant particles. In the case of permanent fouling, we keep track of particles hitting the ocean floor (which is one of our sinks), in which case they are classified as 'sedimented' and removed from the system. Prior bounds for  $f_{pf}$  are set to 1.7–97.0% by comparing previous estimates of plastic seafloor export<sup>7</sup> with the estimated plastic mass at the ocean surface<sup>1</sup>. The remaining fractions are given equal prior probabilities, with the maximum fraction values set to 95%.

The transition matrix contains separate cells for the coastline segments. The probability that plastic particles beach (move from a coastal ocean cell onto the dry land) is parameterized using a beaching timescale  $\tau_{beach}$  (refs. 6,15). The prior probability density function for  $\tau_{beach}$  is defined on the  $\log_{10}$  of the value to cover a wide range of (positively valued) possibilities. Parameter bounds are based on previous findings<sup>6</sup>, with a midpoint estimate of 100 days and a lower bound set to 25 days. Resuspension timescales determining how quickly differently sized plastics move from the beach to the ocean are based on experimental findings<sup>63</sup>. A probability  $p_{removal}$  is defined for plastics being removed from beaches (for example, due to burial<sup>33</sup>, clean-up efforts or direct degradation of plastic material such as oxidation<sup>64</sup>). We use a previously determined removal rate of 0.2% per month as the midpoint estimate<sup>21</sup> and allow it to vary an order of magnitude, capturing the removal rates from other global mass budget studies<sup>40</sup> (0.8–4.0% per month). This is the other 'sink' in which particles are permanently removed from our simulations.

The coastline length inside each grid cell, necessary to calculate litter concentrations per unit length of beach, is computed using the natural Earth dataset<sup>65</sup>. Coastlines have a fractal structure, which can lead to different alongshore lengths in beach surveys compared with the discrete map data. We use a correction factor<sup>40</sup> to account for the 1.27 fractal dimension of coastlines<sup>66</sup>. The typical beach survey resolution is set to 100 m, and the coastline segment resolutions are calculated directly from the natural Earth map data. To account for the fact that less litter might beach in grid cells with only a small amount of coastline, a parameter  $l_{beach,min}$  is introduced. Below this value, the beaching probability decreases linearly down to zero.

We assume fragmentation of plastic items is dominant on beaches due to higher temperatures, oxidation, ultraviolet radiation and mechanical abrasion<sup>20,29,67,68</sup>. Previous studies<sup>69</sup> show that neglecting ocean fragmentation is justified as long as plastics fragment at the same rate or slower in the ocean compared with on beaches. A fragmentation model<sup>21</sup> is used here to simulate how plastic items break down into smaller particles over time. Parameters to be estimated are the fragmentation rate  $\lambda_f$  and the shape factor  $d_N$ , which is used to represent the dimensionality of plastic items<sup>21</sup> (2 for flat objects, 3 for cubes and non-integer values for mixtures of differently shaped objects). For plastic items, the fragmentation rate is still not well known. Parameter bounds for  $\lambda_f$  are based on the experimental data<sup>20</sup> (up to  $1.9 \times 10^{-4} \text{ d}^{-1}$ ) and previous model results<sup>21</sup> (down to  $2.9 \times 10^{-5} \text{ d}^{-1}$ ) and are defined on the  $\log_{10}$  of the value to cover a wide range of possibilities. Bounds for  $d_N$  are based on observational data of plastic particle sizes and masses (Supplementary Information section 2.2). Fragmentation is the third sink for plastic particles in our simulations, where they are removed when reaching a size smaller than 0.1 mm.

In our model, we consider a full size spectrum from 0.1 to 1,600.0 mm, using increments of a factor 2. Lagrangian particle transport is resolved for six sizes (0.1–102.0 mm, 'Lagrangian model' section). For intermediate sizes in the spectrum, the available transition matrices are interpolated linearly. For larger plastics (>0.1 m), similar transport is assumed as these particles remain predominantly at the ocean surface. We model the particle size distribution both in terms of the number of particles and in terms of mass (see ref. 21 for more details). This way, we can quantify which particle size contributes most of the marine plastic pollution. For smaller plastic particles, data are available on typical masses<sup>70,71</sup>. For bigger items, the particle mass  $m_p$  is extrapolated from the particle length  $l_p$  using  $m_p \propto l_p^{d_N}$ , consistent with the fragmentation model. See Supplementary Information section 2.2 for more details.

## Data availability

The datasets generated during the current study are available in the *Utrecht University Yoda* repository with the identifier <https://doi.org/10.24416/UU01-LDAGQN><sup>72</sup>.



## Code availability

Codes used to conduct the experiment are available in the Utrecht University Yoda repository with the identifier <https://doi.org/10.24416/UU01-LDAGQN><sup>72</sup>.

## References

44. van Sebille, E. Adrift.org.au—a free, quick and easy tool to quantitatively study planktonic surface drift in the global ocean. *J. Exp. Mar. Biol. Ecol.* **461**, 317–322 (2014).
45. Wichmann, D., Delandmeter, P., Dijkstra, H. A. & van Sebille, E. Mixing of passive tracers at the ocean surface and its implications for plastic transport modelling. *Environ. Res. Commun.* <https://doi.org/10.1088/2515-7620/ab4e77> (2019).
46. Evensen, G., Vossepoel, F. C. & van Leeuwen, P. J. *Data Assimilation Fundamentals* (Springer, 2022).
47. Kaandorp, M. L. A., Ypma, S. L., Boonstra, M., Dijkstra, H. A. & Van Sebille, E. Using machine learning and beach cleanup data to explain litter quantities along the Dutch North Sea coast. *Ocean Sci.* **18**, 269–293 (2022).
48. Emerick, A. A. & Reynolds, A. C. Ensemble smoother with multiple data assimilation. *Comput. Geosci.* **55**, 3–15 (2013).
49. Delandmeter, P. & van Sebille, E. The Parcels v2.0 Lagrangian framework: new field interpolation schemes. *Geosci. Model Dev.* **12**, 3571–3584 (2019).
50. Gasparin, F. et al. A large-scale view of oceanic variability from 2007 to 2015 in the global high resolution monitoring and forecasting system at Mercator Océan. *J. Mar. Syst.* **187**, 260–276 (2018).
51. Lellouche, J.-M. et al. Recent updates to the Copernicus Marine Service global ocean monitoring and forecasting real-time 1/12 high-resolution system. *Ocean Sci.* **14**, 1093–1126 (2018).
52. Wichmann, D., Delandmeter, P. & van Sebille, E. Influence of near-surface currents on the global dispersal of marine microplastic. *J. Geophys. Res. Oceans* **124**, 6086–6096 (2019).
53. Cunningham, H. J., Higgins, C. & van den Bremer, T. S. The role of the unsteady surface wave-driven Ekman–Stokes flow in the accumulation of floating marine litter. *J. Geophys. Res. Oceans* **127**, e2021JC018106 (2022).
54. van Sebille, E. et al. Lagrangian ocean analysis: fundamentals and practices. *Ocean Model.* **121**, 49–75 (2018).
55. Dietrich, W. E. Settling velocity of natural particles. *Water Resour. Res.* **18**, 1615–1626 (1982).
56. Waldschläger, K. & Schüttrumpf, H. Effects of particle properties on the settling and rise Velocities of microplastics in freshwater under laboratory conditions. *Environ. Sci. Technol.* **53**, 1958–1966 (2019).
57. Lebreton, L. C. M. et al. River plastic emissions to the world's oceans. *Nat. Commun.* **8**, 15611 (2017).
58. *Gridded Population of the World, v.3 (GPWv3): Population Count Grid* (SEDAC, CIESIN, FAO and CIAT, 2005); <https://doi.org/10.7927/H4639MPP>
59. Kroodsma, D. A. et al. Tracking the global footprint of fisheries. *Science* **359**, 904–908 (2018).
60. Jansen, M., van Velzen, U. T. & Pretz, T. *Handbook for Sorting of Plastic Packaging Waste Concentrates* (Food & Biobased Research, 2015).
61. van Emmerik, T., Strady, E., Kieu-Le, T. C., Nguyen, L. & Gratiot, N. Seasonality of riverine macroplastic transport. *Sci. Rep.* **9**, 13549 (2019).
62. Vriend, P. et al. Rapid assessment of floating macroplastic transport in the Rhine. *Front. Mar. Sci.* **7**, 00010 (2020).
63. Hinata, H., Mori, K., Ohno, K., Miyao, Y. & Kataoka, T. An estimation of the average residence times and onshore–offshore diffusivities of beached microplastics based on the population decay of tagged meso- and macrolitter. *Mar. Pollut. Bull.* **122**, 17–26 (2017).
64. Ward, C. P., Armstrong, C. J., Walsh, A. N., Jackson, J. H. & Christopher, C. M. Sunlight converts polystyrene to carbon dioxide and dissolved organic carbon. *Environ. Sci. Technol. Lett.* **6**, 669–674 (2019).
65. Kelso, N. V. & Patterson, T. Introducing Natural Earth data—Naturalearthdata.com. *Geogr. Tech. Special issue* **2010** 82–89 (2010).
66. Husain, A., Reddy, J., Bisht, D. & Sajid, M. Fractal dimension of coastline of Australia. *Sci. Rep.* **11**, 6304 (2021).
67. Kalogerakis, N. et al. Microplastics generation: onset of fragmentation of polyethylene films in marine environment mesocosms. *Front. Mar. Sci.* <https://doi.org/10.3389/fmars.2017.00084> (2017).
68. Efimova, I., Bagaeva, M., Bagaev, A., Kilesol, A. & Chubarenko, P. Secondary microplastics generation in the sea swash zone with coarse bottom sediments: laboratory experiments. *Front. Mar. Sci.* <https://doi.org/10.3389/fmars.2018.00313> (2018).
69. Onink, V., Kaandorp, M. L. A., van Sebille, E. & Laufkötter, C. Influence of particle size and fragmentation on large-scale microplastic transport in the Mediterranean Sea. *Environ. Sci. Technol.* **56**, 15528–15540 (2022).
70. Beck, A. J. et al. Rapid shipboard measurement of net-collected marine microplastic polymer types using near-infrared hyperspectral imaging. *Anal. Bioanal. Chem.* <https://doi.org/10.1007/s00216-023-04634-6> (2023).
71. Egger, M. et al. A spatially variable scarcity of floating microplastics in the eastern North Pacific Ocean. *Environ. Res. Lett.* <https://doi.org/10.1088/1748-9326/abbb4f> (2020).
72. Kaandorp, M. L. A., Lobelle, D., Kehl, C., Dijkstra, H. A. & van Sebille, E. *Global Marine Plastic Mass Budget* (Utrecht Univ., 2023); <https://doi.org/10.24416/UU01-LDAGQN>

## Acknowledgements

This work is part of the ‘Tracking Of Plastic In Our Seas’ (TOPIOS) project, supported through funding from the European Research Council (ERC) under the European Union Horizon 2020 research and innovation programme (grant agreement no. 715386). This work was carried out on the Dutch national e-infrastructure with the support of SURF Cooperative (project no. 16371). We acknowledge S. Schmiz and the ‘AtlantECO’ project (through the European Union’s Horizon 2020 research and innovation programme under grant agreement no. 862923) for preparing part of the surface trawl data and M. Egger and R. de Vries for providing data on plastic concentrations in the Pacific Ocean.

## Author contributions

M.L.A.K. designed and conducted the study, with steering and supervision from E.v.S. and feedback from H.A.D. D.L. contributed to the methodology. C.K. contributed to the OceanParcels software development. All authors made substantial contributions to the manuscript revisions.

## Funding

Open access funding provided by Forschungszentrum Jülich GmbH.

## Competing interests

The authors declare no competing interests.

## Additional information

**Extended data** is available for this paper at <https://doi.org/10.1038/s41561-023-01216-0>.

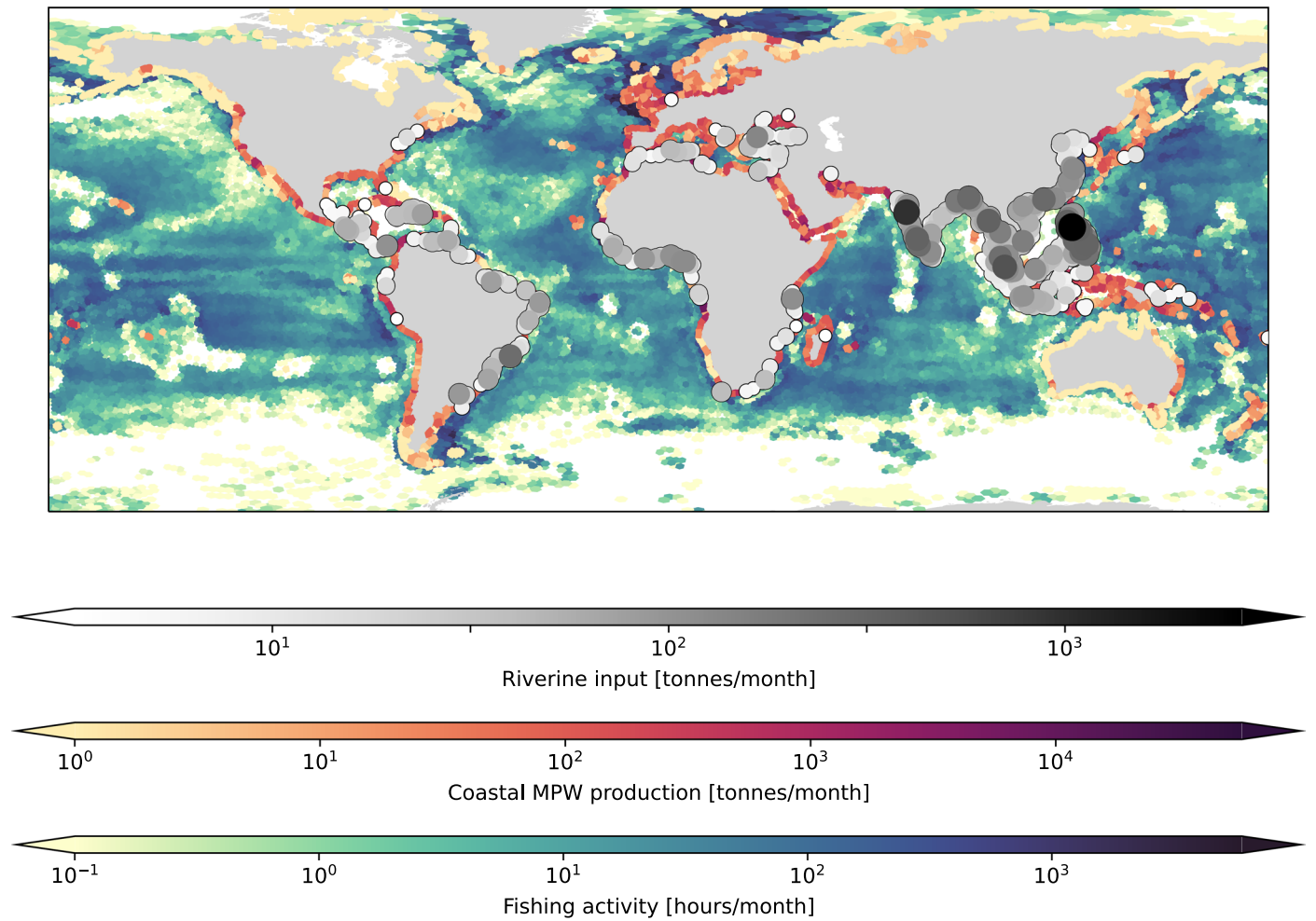
**Supplementary information** The online version contains supplementary material available at <https://doi.org/10.1038/s41561-023-01216-0>.

**Correspondence and requests for materials** should be addressed to Mikael L. A. Kaandorp.

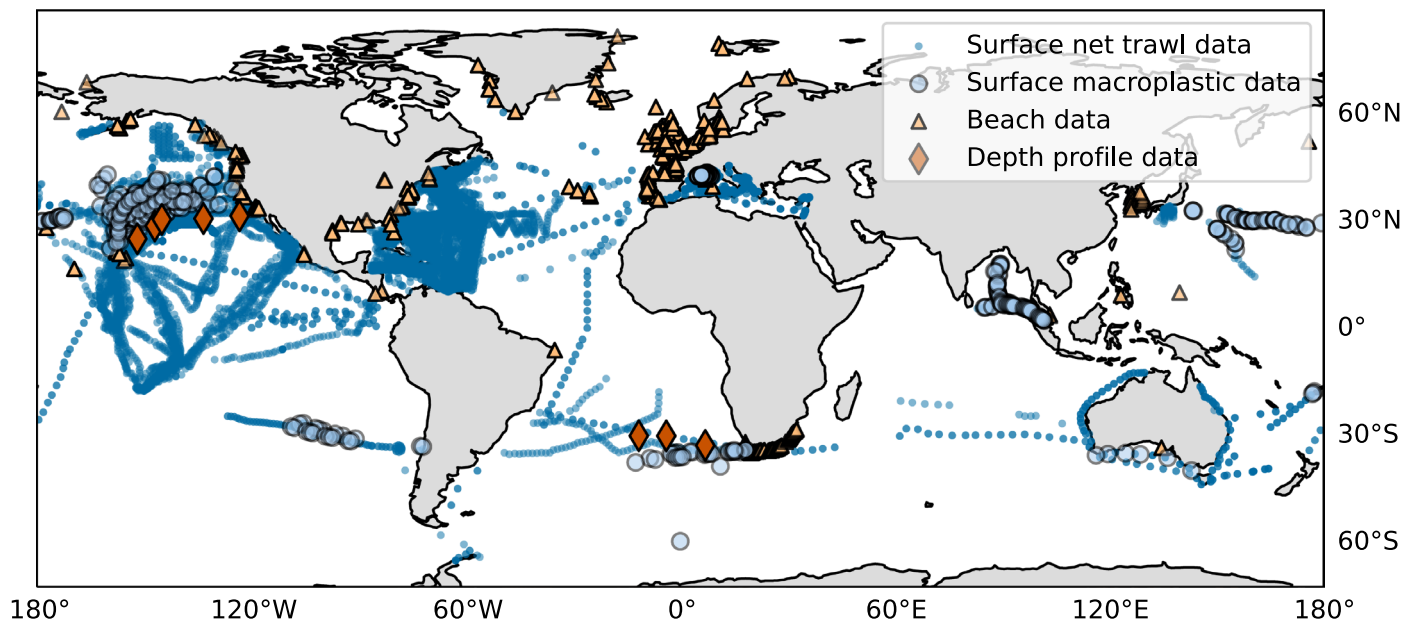
**Peer review information** *Nature Geoscience* thanks Robin de Vries, Kryss Waldschläger and the other, anonymous, reviewer(s) for their contribution to the peer review of

this work. Primary Handling Editors: Rebecca Neely and James Super, in collaboration with the *Nature Geoscience* team.

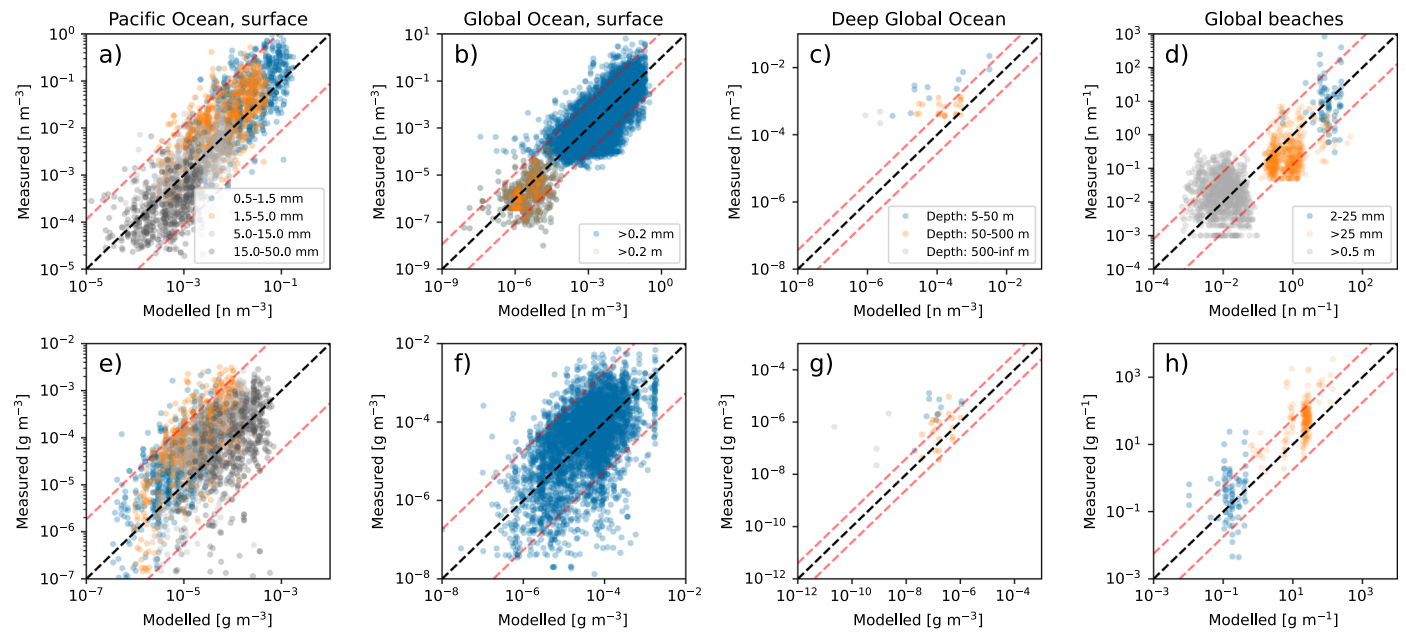
**Reprints and permissions information** is available at [www.nature.com/reprints](http://www.nature.com/reprints).



**Extended Data Fig. 1 | Three major sources of marine plastic pollution.** Rivers<sup>3</sup>, shown using grey to black circles; coastal mismanaged plastic waste<sup>4</sup>, shown in red to purple; and fishing activity<sup>59</sup>, shown in blue.



**Extended Data Fig. 2 | Observational data across different marine reservoirs used to assimilate into the numerical model.** The markers show the locations of the available observational data, from neuston net measurements at the ocean surface (blue dots), visual observations of large plastic items (>0.2m, blue circles), the deep ocean (orange diamonds), and beaches (orange triangles).



**Extended Data Fig. 3 | Scatter plots for modelled versus measured plastic concentrations. a, e,** Measurements for separate size classes at the ocean surface<sup>35,72</sup>. **b, f,** Measurements for small plastics ( $>0.2 \text{ mm}$ ) and large plastics ( $>0.2 \text{ m}$ ) at the ocean surface. **c, g,** measurements below 5 m depth. **d, h,** Measurements from beaches. **a–d,** Number concentrations ( $n \text{ m}^{-3}$  in the ocean

and  $n \text{ m}^{-1}$  on beaches). **e–h,** Mass concentrations ( $\text{g m}^{-3}$  in the ocean and  $\text{g m}^{-1}$  on beaches). The 1:1 line is shown using the dashed black line, the expected amount of measurement error ( $\pm 2\sigma$ ) is shown using the dashed red lines. The Pearson R correlation coefficients between the modelled and measured concentrations are given in the supplementary information, Table S1.

**Extended Data Table 1 | Overview of the observational data used to calibrate the numerical model**

Reference	Measurement type	Notes
[2]	Net trawls, surface ocean	Compilation of 37 measurement campaigns for small plastic particles (>0.335 mm) in terms of mass and number, 11,854 data in total
[6]	Net trawls, surface ocean	Compilation of 18 measurement campaigns for small plastic particles in the Mediterranean Sea (>0.335 mm) in terms of mass and number, 1170 data in total
[25, 72]	Net trawls, surface ocean	Data on 4 size classes available in terms of mass and number, 1390 data in total
[25, 77]	Net trawls, deep ocean	Data on 4 size classes available in terms of mass and number, 120 data in total
[1]	Visual observations, surface ocean	Visual detection for large plastics (>0.2 m) in terms of number, 553 data in total
[76]	Visual observations, surface ocean	Automatic floating object detection for large plastics (>0.5 m) in terms of number, 10 data in total
[38]	Beach measurements	OSPAR data (>0.5 m) in terms of number, 1692 data in total
[39]	Beach measurements	MDMAP data (>25 mm) in terms of number, 5022 data in total
[47, 78–80]	Beach measurements	Additional beach measurements in terms of mass, 238 data in total
[81]	Beach measurements	Data on small plastics (2–25 mm) in terms of mass and number, 162 data in total

To account for the fact that net trawl data can be biased due to wind mixing, the Kukulka correction factor<sup>74</sup> is applied using ERA5 reanalysis wind speeds<sup>75</sup>. Data for large plastic items at the ocean surface (>0.2 m) come from previous studies using visual observations<sup>176</sup>. For beach measurements, MDMAP<sup>39</sup> and OSPAR<sup>38</sup> observations are included in terms of  $n\ m^{-1}$ , focusing on larger plastic items (>25 mm and >500 m respectively). These datasets contain information on the type of litter items. Plastic litter types containing words such as 'fish', 'rope', or 'net' are categorized as fishing related items, which is used to calculate a minimum percentage of fishing related plastics per measurement location.